High-Pressure Phase Equilibria of Carbon Dioxide + 1,4-Dioxane Binary System

Sergiu Sima, Catinca Secuianu, Dan Vladimir Nichita

High-Pressure Phase Equilibria of Carbon Dioxide + 1,4-Dioxane Binary System

Sergiu Sima[1], Catinca Secuianu[1,2*], Dan Vladimir Nichita[3*]

[1]*Department of Inorganic Chemistry, Physical Chemistry and Electrochemistry, Faculty of Applied Chemistry and Materials Science, University "Politehnica" of Bucharest, 1-7 Gh. Polizu Street, S1, 011061 Bucharest, Romania, catinca.secuianu@upb.ro*

[2]*Department of Chemical Engineering, Imperial College London, South Kensington Campus, SW7 2AZ London, United Kingdom, c.secuianu@imperial.ac.uk*

[3]*CNRS UMR 5150, Laboratoire des Fluides Complexes et leurs Réservoirs, Université de Pau et des Pays de l'Adour, 64013 Pau, France*

ABSTRACT

New isothermal vapor–liquid equilibrium (VLE) data for the carbon dioxide + 1,4-dioxane system are reported at four temperatures (323.15, 333.15, 343.15, and 353.15) K and pressures up to 122.7 bar. The critical curve was also measured up to 158.8 bar and 420.15 K. Phase behavior measurements were performed in a high-pressure windowed cell with variable volume, using a static-analytical method with phases sampling by rapid online sample injectors (ROLSI) coupled to a gas chromatograph (GC) for analysis. The experimental results of this study are compared with the scarce available literature data. The new and all available literature data for the carbon dioxide + 1,4-dioxane binary system are modelled with the cubic Soave–Redlich–Kwong (SRK) and Peng–Robinson (PR) equations of state (EoS) with classical van der Waals mixing rules (two-parameter conventional mixing rules, 2PCMR). The modelling showed that SRK and PR models can accurately predict the phase behavior of the system studied.

Keywords: Phase equilibria; Carbon Dioxide; 1,4-Dioxane; High-pressures; EoS (SRK, PR)

1. Introduction

In the last years, we started a project [1] to investigate possible physical solvents for carbon dioxide capture, motivated by the Earth's air temperature fast increase conjugated with alterations in weather patterns, generated by the increasing carbon dioxide concentration in the atmosphere, which has led to a rise in the number and strength of natural disasters all over the world, such as floods, droughts, hurricanes, wide spread melting of ice and snow,

* Corresponding author: catinca.secuianu@upb.ro (C. Secuianu)
* Corresponding author: dnichita@univ-pau.fr (D.V. Nichita)

and an increase in average sea levels [2-3]. So far, we investigated phase equilibria for systems containing carbon dioxide and different classes of organic substances, to illustrate the functional group effect on the solvent ability to dissolve CO_2, such as alcohols [4-26], alkanes [27-31], ethers [32-33], or esters [34]. Despite the importance and need for accurate experimental data [35], some of these classes received less attention in the literature [37-41].

This is the case for the carbon dioxide (1) + 1,4-dioxane (2) binary system, for which sparse data at high-pressures are available in the open literature [42-45]. 1,4-Dioxane is a colorless hygroscopic liquid with a faint sweet odor belonging to heterocyclic organic compounds, classified as an ether. It is used as a stabilizer for chlorinated solvents such as trichloroethane and trichloroethylene [46]. 1,4-Dioxane can also be an unintended contaminant of drinking water and foods, which may also contain small amounts from some additives and packaging materials, or chemical ingredients used in consumer products including laundry detergent, soap, bubble bath, shampoo, skin cleanser, adhesives, and antifreeze [46]. On the other hand, 1,4-dioxane is used in a variety of applications as a solvent in polymerization industries, catalysis, extractions, homogeneous reactions, pharmaceutical industry, or clathrate hydrates [47-52].

Cocerning available high-pressures phase equilibrium measurements, Kassim et al. [53] measured the solubility of carbon dioxide in 1,4-dioxane at four temperatures at atmospheric pressure, Kordikowski et al. [42] determined the liquid phase compositions, densities, and volume expansions at 298.15 K, 303.15 K, and 313. 15 K and pressures up to 71.4 bar, Chester and Haynes [43] reported pressure–temperature coordinates of critical points, Miller et al. [44] presented liquid phase compositions at 298.15 K, and Tiwikrama et al. [45] reported bubble- and dew points at different pressures for two isotherms (343.2 K and 353.2 K). The available critical and VLE data are summarized in **Table 1**, together with the experimental methods [37-41], as usually done in our previous papers [25-26,32]. It must be noted that, in addition to the experimental methods in these references (which are mentioned using the same description as Dohrn and co-workers [37-41], except for Kassim et al. [53]), the purity of chemicals is also mentioned, if available. It can be easily observed that, not only the methods used by other researchers are not the same, but the purity of chemicals is also different. Both methods and purities could be the reasons for the scatter of open literature data [54].

In this work, we report vapor–liquid equilibrium data for the carbon dioxide (1) + 1,4-dioxane (2) binary system at four temperatures: 323.15 K, 333.15 K, 343.15 K, and 353.15 K

and pressures up to 122.7 bar, as well as the liquid–vapor critical curve, including the critical composition.

The new data and all the literature ones at high pressures were then modeled with two cubic equations of state. The Soave–Redlich–Kwong (SRK) [55] and Peng–Robinson (PR) [56] equations of state with quadratic classical van der Waals mixing rules (two-parameter conventional mixing rules, 2PCMR) were used to model the carbon dioxide + 1,4-dioxane binary system. It must be remarked that the other investigators of this system chose to only correlate the isothermal data summarized in **Table 1**. Our approach is different and presents the global phase behavior of the system, namely vapor–liquid critical curve and isotherms. The models we used describe type I or type II phase behavior, according to the classification of Van Konyneburg and Scott [57] or Privat and Jaubert [58]. Type I phase behavior is characterized by a continuous liquid–vapor critical curve connecting the critical points of pure components, as sketched in **Fig. 1a**, while type II phase behavior (**Fig. 1b**) has an additional liquid–liquid (LL) critical curve, intersecting the three-phase liquid–liquid–vapor equilibrium (LLV) line in an upper critical endpoint (UCEP). As there is no experimental evidence of type II phase behavior, it can be assumed that the system belongs to type I phase behavior.

Table 1.

Literature critical and VLE data for CO_2 (1) +1,4-Dioxane (2) binary system

***T* or T_{range}/K**	***p or* p_{range}/bar**	**NEXP[a]**	**Obs.**	**Method**	**Purity[c]**		**Ref.**
					CO_2	**$C_4H_8O_2$**	
304.25÷587.15	73.8 ÷ 52.1	14	LV critical curve	OthPcTc	SFC/SFE grade	reagent grade	[43]
298.15	8.2 ÷ 52.1	10	*p* – *x*	AnTX	0.9990	min. 0.9900 mol	[42]
298.15	6.17 ÷ 32.35	8	*p* – *x*	SynVisVar	0.9999	anhydrous, 0.9980 mass	[44]
303.15	1.01325	1	*p* – *x*	FFFT[b]	> 0.9999	> 0.9999	[53]
303.15	4.3 ÷ 59.1	18	*p* – *x*	AnTX	0.9990	min. 0.9900 mol	[42]
313.15	5.3 ÷ 71.4	18	*p* – *x*	AnTX	0.9990	min. 0.9900 mol	[42]
313.15	1.01325	1	*p* – *x*	FFFT	> 0.9999	> 0.9999	[53]
323.15	1.01325	1	*p* – *x*	FFFT	> 0.9999	> 0.9999	[53]
333.15	1.01325	1	*p* – *x*	FFFT	> 0.9999	> 0.9999	[53]
343.20	26.0 ÷ 111.9, 110.7 ÷ 101.5	9, 3	*p* – *x*, *p* – *y*	SynVisVar	0.9950	0.9900	[45]
353.20	27.5 ÷ 118.9, 121.5 ÷ 102.0	7, 5	*p* – *x*, *p* – *y*	SynVisVar	0.9950	0.9900	[45]

[a]Number of experimental points; [b]Falling-film flow technique; [c]As mentioned in the corresponding reference

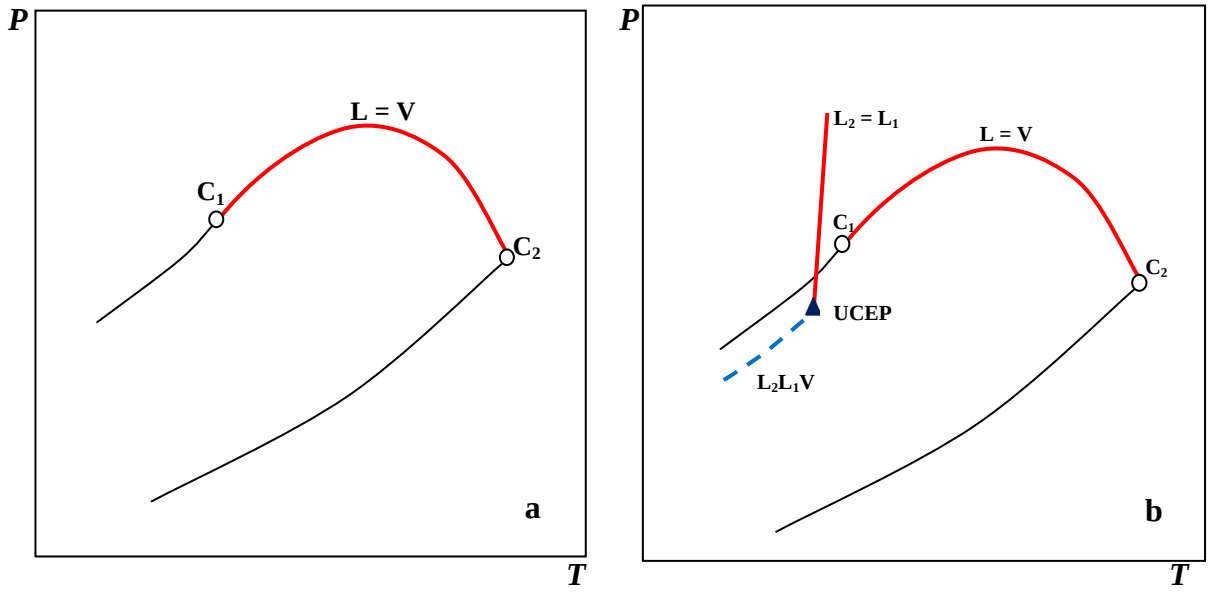

Fig. 1. Sketch of *P*–*T* projection for type I (**a**) and type II (b) phase diagram: C_1, C_2, critical points of pure components; L_1, L_2, liquid phases (1, 2 subscripts refer to the number of phases), V, vapor phase.

2. Experimental Section

2.1. Materials.

Carbon dioxide (mass fraction purity min. 0.99995) was provided by Linde Gaz Romania, and 1,4-dioxane (anhydrous, mass fraction purity > 0.998) was purchased from Sigma-Aldrich, as reported in **Table 2**. The chemicals were used without further purification, but we paid special attention to correct manipulation of anhydrous 1,4-dioxane. The purity of 1,4-dioxane was also checked and confirmed by gas chromatography.

Table 2

Description of Materials

Compound	**Chemical formula**	**CAS Registry Number**	**Source**	**Purification method**	**Minimum mass fraction purity**
Carbon dioxide	CO_2	124-38-9	Linde Gaz Romania	None	0.99995
1,4-Dioxane	C_4H_8O2	123-91-1	Sigma-Aldrich	None	anhydrous, $ZerO_2^{®}$, 0.998

2.2. Apparatus and procedure.

The experiments were performed using the same phase equilibrium apparatus previously presented in detail in Refs. [4-5]. The measurements were done using the static-analytical method with liquid- and vapor- phase sampling. The main component of the phase equilibrium apparatus is the high-pressure windowed cell with variable volume, coupled with a sampling and analyzing system [59]. The sampling system consists of two high-pressure electromechanical sampling valves, namely the rapid on-line sampler injector (ROLSI^{TM}, MINES ParisTech/CEP-TEP – Centre énergétique et procédés, Fontainbleau, France [60]). The ROLSI valves are connected to the equilibrium visual cell and to a gas chromatograph (GC) through capillaries. The expansion chamber of the sampler injector is heated with a heating resistance, so the liquid samples are rapidly vaporized. A linear resistor coupled to an Armines/CEP/TEP regulator is used to heat the transferring lines between ROLSI and the GC. The GC (Perichrom) is equipped with a thermal conductivity detector, TCD, and a HP-Plot/Q column 30 m long and 0.530 mm diameter. Helium is the GC carrier gas at a flow rate of 30 mL/min. The setup is completed with a syringe pump Teledyne ISCO model 500D. As the working procedure is similar as in our previous papers [4-5,59], here it will be only briefly described. Firstly, the entire internal loop of the apparatus including the equilibrium

cell is rinsed several times with carbon dioxide. Then, a vacuum pump is used to evacuate the equilibrium cell. The cell is charged with the organic substance, which is previously degassed by using a vacuum pump and vigorously stirring. The lighter component (in this case CO_2) is filled with the syringe pump into equilibrium cell and the pressure is set to the desired value. Then the cell is heated to the experimental temperature. The mixture in the cell is stirred for a few hours to facilitate the approach to an equilibrium state. Then the stirrer is switched off for about 1 h, until the coexisting phases are completely separated. Samples of the liquid and vapor phases are withdrawn by ROLSI and analyzed with the GC. At least six samples of the liquid phase are normally analyzed to check the repeatability, at the equilibrium temperature and pressure. The sample sizes being very small, the equilibrium pressure in the cell remains constant.

The calibration of the TCD for CO_2 and 1,4-dioxane is done by injecting known amounts of each component using gas chromatographic syringes. Calibration data are fitted to quadratic polynomials to obtain the mole number of the component versus chromatographic area. The correlation coefficients of the GC calibration curves were 0.999 for carbon dioxide and 0.998 for 1,4-dioxane.

The uncertainties in all variables and properties were estimated as explained in our previous papers [22,23].

The platinum temperature probe connected to a digital indicator was calibrated against the calibration system Digital Precision Thermometer with PT 100 sensor (Romanian Bureau of Legal Metrology). The uncertainty of platinum probe is estimated to be within ± 0.1 K using a similar procedure to that described in Ref. [22].

The pressure transducer connected to a digital multimeter was calibrated at 323.15 K with a precision hydraulic dead-weight tester (model 580C, DH-Budenberg SA, Aubervilliers, France). The uncertainty of the pressures is estimated to be within ± 0.015 MPa using a similar procedure as described in Ref. [22], for a pressure range between 0.5 and 20 MPa.

The critical points were measured in this work using the following procedure [61]. We start with a homogenous phase for which we analyze the composition at random temperature and pressure. The pressure is modified by varying the volume of the cell with the manual pump in order to determine if we obtain a bubble or a dew point. If we obtain a bubble point, the temperature is slowly increased until the first dew point is observed, then the pressure is increased to a homogeneous phase and the composition is determined by sampling. Then the

pressure is very slowly decreased until the first drops of liquid are observed. At this point, the temperature is slowly decreased simultaneously with reducing the volume, so the system is at the limit between homogeneous (single phase)-heterogeneous (two phases). The decreasing of temperature continues until the first gas bubbles are observed. The procedure is then repeated by introducing new amounts of CO_2 and slowly cooling.

3. Modeling

The phase behavior of the carbon dioxide (1) + 1,4-dioxane (2) binary system was modeled with the Soave–Redlich–Kwong (SRK) [55] and Peng–Robinson (PR) [56] EoS, coupled with classical van der Waals mixing rules (two-parameter conventional mixing rules, 2PCMR).

The Soave–Redlich–Kwong [55] equation of state is:

$$P = \frac{RT}{V-b} - \frac{a(T)}{V(V+b)} \tag{1}$$

where the two constants, *a* and *b*, are:

$$a = 0.42748 \frac{R^2 T_c^2}{P_c} \alpha(T) \tag{2}$$

$$b = 0.08664 \frac{RT_c}{P_c} \tag{3}$$

$$\alpha(T_R, \omega) = \left[1 + m_{SRK}\left(1 - T_R^{0.5}\right)\right]^2 \tag{4}$$

$$m_{SRK} = 0.480 - 1.574\,\omega - 0.176\,\omega^2 \tag{5}$$

The Peng–Robinson [56] equation of state is:

$$P = \frac{RT}{V-b} - \frac{a(T)}{V(V+b)+b(V-b)} \tag{6}$$

where the two constants, *a* and *b*, are:

$$a = 0.45724 \frac{R^2 T_c^2}{P_c} \alpha(T) \tag{7}$$

$$b = 0.077796 \frac{RT_c}{P_c} \tag{8}$$

$$\alpha(T_R, \omega) = \left[1 + m_{PR}\left(1 - T_R^{0.5}\right)\right]^2 \tag{9}$$

$$m_{\mathrm{PR}} = 0.37464 - 1.54226\omega - 0.26992\omega^2 \tag{10}$$

The two-parameter conventional mixing rules are given by:

$$a = \sum_{\mathrm{i}} \sum_{\mathrm{j}} x_{\mathrm{i}} x_{\mathrm{j}} a_{\mathrm{ij}} \tag{11}$$

$$b = \sum_{\mathrm{i}} \sum_{\mathrm{j}} x_{\mathrm{i}} x_{\mathrm{j}} b_{\mathrm{ij}} \tag{12}$$

where

$$a_{\mathrm{ij}} = \sqrt{a_{\mathrm{i}} a_{\mathrm{j}}}\left(1 - k_{\mathrm{ij}}\right) \tag{13}$$

$$b_{\mathrm{ij}} = \frac{b_{\mathrm{i}} + b_{\mathrm{j}}}{2}\left(1 - l_{\mathrm{ij}}\right) \tag{14}$$

Although an updated version of the generalized Soave α-function was recently proposed [62], suitable for both Soave-Redlich–Kwong and Peng–Robinson equations of state, the original temperature function $\alpha(T_{\mathrm{r}})$ was used for both SRK [55] and PR EoSs [56], for sake of comparison with previous research.

Table 3

Critical parameters (T_{c}, P_{c}, V_{c}), acentric factor (ω) for pure compounds

Database/ Source	**Compounds**							
	Carbon dioxide				1,4-Dioxane			
	***T*c/K**	***P*c/bar**	***V*c/cm·mol^{-1}**	***ω***	***T*c/K**	***P*c/bar**	***V*c/cm^3·mol^{-1}**	***ω***
DBB [63]	304.20	73.77	94.00	0.2252	587.00	52.08	238.00	0.288
Reid et al. [64]	304.10	73.80	93.90	0.239	587.00	52.10	238.00	0.281
Poling et al. [65]	304.12	73.74	94.07	0.225	587.00	51.70	238.00	-
NIST [66]	304.13	73.77	91.90	0.22394	587.15	51.90	239.00	0.274[a]
Yaws [67]	304.19	73.82	94.00	0.228	587.00	52.08	238.00	0.280
DIPPR [68]	304.21	73.83	93.90	0.223621	587.00	52.08	238.00	0.279262
Kordikowski et al. [42]	304.20	73.80	-	0.225	587.40	52.10	-	0.281
Tiwikrama et al. [45]	304.20	73.80	-	0.225	587.20	51.70	-	0.274

The values of critical parameters and the acentric factors of pure components are of equal importance. Generally, we are using the values provided by the DIPPR database [68], as also recommended by other researchers [69]. However, for this system we performed calculations with the parameters from different database/sources (**Table 3**), as we noticed that other

groups that had investigated the carbon dioxide + 1,4-dioxane used various combinations of these parameters. The values of critical parameters and acentric factors of the pure components considered in this study, as well as those used by the other researchers are given in **Table 3**. Thus, while Kordikowski et al. [42] cited generally both the Dortmund Data Bank 1993 (DBB) [63] and Reid et al. [64] for the critical temperatures, pressures, and acentric factors for carbon dioxide and 1,4-dioxane, Tiwikrama et al. [45] combined the critical pressure provided by Reid et al. [64], critical temperature from Kordikowski et al. [42], and acentric factor from Poling et al. [65] for carbon dioxide and NIST's values for 1,4-dioxane.

It must pointed out that we excluded from comparisons three of the references presented in **Table 1**, as the modeling performed by Kassim et al. [53] was at atmospheric pressure with the Redlich-Kwong (RK) equation of state, Miller et al. [44] used the COSMOtherm approach, and Chester and Haynes [43] did not model their VLE critical data.

Kordikowski et al. [42] modeled their three isotherms (298.15 K, 303.15 K, and 313.15 K) using PR/2PCMR with temperature independent parameters (k_{12} = -0.05, l_{12} = -0.05), while Tiwikrama et al. [45] also correlate their data (343.2 K and 353.2 K) with PR/2PCMR. Although the latter provide one set of optimized binary interaction parameters (BIPs), k_{12} = -0.0606 and l_{12} = -0.0475, respectively, it is unclear if their optimization is temperature independent, as they report absolute average deviations in pressure for each temperature and not comparing the calculation results of their optimization with all available data.

The modeling approach in our case is mainly similar to that reported in our recent papers [25,26,32]. Thus, instead of just correlating the experimental data at specified temperatures, we modeled both the critical curve and isotherms with SRK and PR EoSs. In addition, we studied the influence of critical parameters and acentric factors of pure components when correlating the data with PR EoS.

The calculations were performed using two software, our in-house software package ***PHEQ*** (**Ph**ase **Eq**uilibria Database and Applications) [70] and GPEC (Global Phase Equilibrium Calculations) [71]. The method proposed by Heidemann and Khalil [72] with the numerical derivatives given by Stockfleth and Dohrn [73] is implemented in the module for calculating the critical curve, called CRITHK in our software.

The first step in our three-fold modeling procedure was to regress both the new experimental and open literature data with PR EoS at each temperature, using all the critical parameters and acentric factors from **Table 3**. We also calculated the critical curves using the

average values of optimized BIPs and those obtained by Kordikowski et al. [42] and Tiwikrama et al. [45].

The next step was to correlate all data with SRK using the parameters for pure components from DIPPR database [68].

Finally, as the experimental data are very scattered, we selected only those in agreement and we averaged the optimized binary interaction parameters, k_{12} and l_{12}, for each EoS, resulting unique sets of k_{12} and l_{12}. These sets were finally used to calculate semi-predictively the phase behavior of the system (critical curve and isotherms).

4. Results and Discussion

4.1. Experimental results

Vapor–liquid equilibrium compositions for the carbon dioxide + 1,4-dioxane binary system were measured at four temperatures (323.15 K, 333.15 K, 343.15 K and 353.15 K), and pressures up to 122.7 bar. The data are presented in **Table 4** and, as commonly in the literature, mole fractions are reported with four decimal places. We also measured the critical curve starting from the critical point of carbon dioxide up to 420.15 K and 158.8 bar, which is almost the critical pressure maximum (CPM) and the data are presented in **Table 5**.

Table 4

Mole fraction of component 1 in the liquid phase, X_1, and mole fraction of component 1 in the vapor phase, Y_1 at various temperatures, T, and pressures, P, for the binary system carbon dioxide (1) + 1,4-dioxane (2).

***P*/bar**	X_1	Y_1	***P*/bar**	X_1	Y_1
T/K = 323.15 ± 0.1					
10.2	0.2371	0.9844	60.5	0.8041	0.9973
20.5	0.4436	0.9962	70.6	0.8585	0.9964
30.5	0.5634	0.9973	80.5	0.8903	0.9956
40.7	0.6652	0.9975	94.6	0.9805	0.9805
50.2	0.7330	0.9976			
T/K = 333.15 ± 0.1					
10.8	0.2120	0.9802	60.3	0.7387	0.9964
20.8	0.3599	0.9881	70.6	0.7883	0.9961
30.1	0.4745	0.9951	80.6	0.8290	0.9959
40.6	0.5770	0.9962	90.8	0.8729	0.9945
50.3	0.6682	0.9963	104.9	0.9639	0.9639
T/K = 343.15 ± 0.1					
10.5	0.1944	0.9692	70.3	0.7309	0.9908
20.3	0.3073	0.9847	80.2	0.7722	0.9851
30.3	0.4218	0.9876	90.2	0.8201	0.9896
40.2	0.5182	0.9888	100.6	0.8567	0.9841
50.1	0.6109	0.9900	111.6	0.9024	0.9737
60.2	0.6755	0.9902	113.1	0.9555	0.9555
T/K = 353.15 ± 0.1					
10.6	0.1736	0.9521	70.5	0.6898	0.9870
20.6	0.2911	0.9738	80.4	0.7313	0.9865
30.3	0.3955	0.9855	90.0	0.7750	0.9860
40.3	0.4866	0.9865	100.4	0.8141	0.9851
50.2	0.5621	0.9871	110.8	0.8565	0.9729
60.6	0.6381	0.9872	122.7	0.9366	0.9366

Standard uncertainties: $u(T)$ = 0.1 K, $u(P)$ = 0.1 bar, $u(X_1)$ = 0.001, $u(Y_1)$ = 0.005

All four new isotherms are measured in the supercritical region of carbon dioxide and are compared with available data when possible. **Fig. 2** illustrates the comparison of our data measured at 343.15 K and 353.15 K with those of Tiwikrama et al. [45] at 343.2 K and 353.2 K, who report bubble- (9 and 7 points, respectively) and dewpoints (3 and 5 points, respectively) but at different pressures. It can be easily spotted that the liquid phase compositions do not agree, the difference in the carbon dioxide molar fraction at the same pressure is almost 0.2 at low and medium pressures, our measurements indicating a higher solubility of CO_2 in 1,4-dioxane than those of Ref. [45]. However, with increasing pressure, the difference is smaller, and the critical pressure is almost the same, while the critical composition is higher in our case, as expected. Moreover, the vapor phases cannot be properly compared, as Ref. [45] reports only few points at higher pressures towards the critical region. It must be noted that besides the different methods of investigation, the purity of substances must be considered, including the correct manipulation of 1,4-dioxane, which is hydrophilic [46], as possible causes for the observed differences.

Table 5
Critical points data carbon dioxide (1) + 1,4-dioxane (2)[a]

T/K	P/bar	X_1
587.00[b]	52.08[b]	0[b]
420.15	158.8	0.8411
408.65	155.1	0.8607
397.55	150.6	0.8841
389.75	147.3	0.8977
375.25	140.1	0.9127
363.65	131.1	0.9283
355.05	123.8	0.9358
353.15	122.7	0.9366
343.15	113.1	0.9555
342.35	112.7	0.9562
333.15	104.9	0.9639
323.15	94.6	0.9805
304.21	73.83	1

[a] $u(T)$ = 0.1 K, $u(P)$ = 0.1 bar, $u(X_1)$ = 0.001

[b] DIPPR [68] values

The other four available isotherms from both Kordikowski et al. [42] and Miller et al. [44] are measured at lower temperatures (**Table 1**) and only the liquid phase is reported. In **Fig. 3** we compared the 298.15 K, 303.13 K, and 313,15 K isotherms measured by Kordikowski et al. [42] with that measured at 298.15 K by Miller et al. [44]. The data seem to

agree reasonably well, though some scatter can be observed at pressures lower than 20 bar for the data reported in Ref. [42]. When plotting all data (**Fig. 1S**.), it can be observed that our data are in better agreement with those reported by Kordikowski et al. [42] and Miller et al. [44].

In **Fig. 4** we compared the new critical data with those reported by Chester and Haynes [43]. The data are in good agreement, but at higher temperatures, closer to that corresponding to the CPM, the difference in pressure is about 4 bar.

4.2. The influence of critical parameters and acentric factors of pure components

The new and all available literature data were correlated with PR/2PCMR using the critical parameters and acentric factors from **Table 3**, whilst the differences are relatively small. Although the average absolute deviations in bubble-point pressures (AADP, %) are very similar for all sets of critical parameters and acentric factors from **Table 3** at each temperature, the values of optimized binary interaction parameters are significantly different (**Table 1S** in Supplementary information). It can be noticed that for the small number of data available, the combination of critical parameters and acentric factors for pure components used by Tiwikrama et al. [45] leads generally to the lowest optimal values of BIPs, while the critical parameters and acentric factors from Reid et al. [64] lead to the highest errors in in bubble-point pressures. The average absolute deviations in bubble-point pressures (AADP, %) and the average absolute deviations in the vapor-phase compositions (AADY, %) are calculated using the following equations:

$$AADP(\%) = \frac{1}{N_{\exp}} \sum_{i=1}^{N_{\exp}} \left| \frac{P_i^{\exp} - P_i^{calc}}{P_i^{\exp}} \right| \times 100 \qquad (15)$$

$$AADY(\%) = \frac{1}{N_{\exp}} \sum_{i=1}^{N_{\exp}} \left| Y_i^{\exp} - Y_i^{calc} \right| \times 100 \qquad (16)$$

It can be also observed that even though the experimental data measured at 298.15 K by Kordikowski et al. [42] and Miller and et al. [44] agree very well, the optimized values of BIPs are quite different, regardless the critical parameters and acentric factors of pure components. Also the AADP values are the highest for the data reported by [42] at 313.15 K. Therefore, we regressed the combined set of data at 298.15 K from Kordikowski et al. [42] and Miller et al. [44]. This set was considered in the next steps of modeling.

As the correlations of VLE data do not point to definitive conclusions regarding the influence of pure components parameters, we used the average of optimal BIPs calculated with each of the eight sets (**Table 3**) of critical parameters and acentric factors of pure components to calculate the critical curves. It must be noted that Poling et al. [65] do not provide a value for the acentric factor of 1,4-dioxane and the value from Reid et al. [64] was used. The average values of the optimal BIPs, the type of phase behavior, the critical pressure maxima, and the corresponding temperatures are given in **Table 2S** in Supplementary information. All sets lead to type I phase behavior and the values of the critical pressure maximum (CPM) are close to the experimental ones reported in this paper. However, the corresponding critical temperature is underestimated by about 5 K. We also performed the same calculations excluding the two isotherms measured by Tiwikrama et al. [45] and the results are presented in **Table 3S** in the Supplementary information. Although the changes in average BIPs are relatively small, when excluding the data reported in Ref. [45], the critical pressure maximum decreases with about 1 bar and the corresponding temperature with 2-3 K, shifting the CPM to the left.

Furthermore, we calculated the critical curves using the values of optimized BIPs provided by Kordkowski et al. [42], k_{12} = -0.05, l_{12} = -0.05, and by Tiwikrama et al. [45], k_{12} = -0.0606, l_{12} = -0.0475, respectively and the critical parameters and acentric factors from all sources mentioned in **Table 3**. Regardless the critical properties and acentric factors used, both sets of BIPs lead to a type II phase behavior. This can be observed in **Figs. 5** and **6** where we compared the global phase diagrams calculated with the optimal BIPs from Kordikowski et al. [42] and critical parameters and acentric factors of pure components from Refs. [42] and [68], and from Kordikowski et al. [42] and Tiwikrama et al. [45] with critical parameters and acentric factors of pure components, as they reported, respectively. The critical pressure maxima are ranging from 163 bar to 168 bar and the corresponding temperatures between 431 K and 435 K, as can be seen in **Table 4S** in Supplementary information. It must be remarked that the set of BIPs from Ref. [45] lead to CPM values close to the experimental reported by Chester and Haynes [43] and the predicted UCEPs are located at lower temperatures than those predicted using the BIPs from Ref. [42].

4.3. SRK/2PCMR results

The new and all literature data were also correlated with SRK EoS coupled with classical van deer Waals mixing using the critical parameters and acentric factors from DIPPR [68] for both carbon dioxide and 1,4-dioxane. The values of the optimized binary interaction

parameters (k_{12}, l_{12}), and the corresponding minimum values for the objective function (Fob), number of experimental points (N_{EXP}), number of convergent points (N_{CONV}), average absolute deviations in bubble-point pressures (AADP, %), and the average absolute deviations in the vapor-phase compositions (AADY, %) are recorded in **Table 6**. Both optimal BIPs and AADP are generally higher than those obtained when regressing the data with PR/2PCMR and critical parameters and acentric factors from DIPPR [68]. The correlation results by both SRK and PR with the pure components critical parameters and acentric factors from Ref. [68] are compared with our data in **Figs. 7** and with literature data in **Fig. 8**. The models behave similarly and the calculation results agree very well with the experimental data, with a slight overestimation of critical points with increasing temperature. As the optimized binary interaction parameters for the 343.20 K and 353.20 K [45] isotherms lead to type II phase behavior when calculating the global phase diagram, they were excluded from the average of optimal BIPs. Thus, the average values of the optimized BIPs with SRK/2PCMR are k_{12} = -0.1479 and l_{12} = -0.0478 and they were further used to calculate the global phase behavior (critical curves and isotherms).

Table 6
SRK/2PCMR results for new and literature data using the pure components critical parameters from DIPPR database [68].

T/K	k_{12}	l_{12}	F_{ob}	N_{EXP}	N_{CONV}	AADP, %	AADY, %	Ref
298.15	-0.0298	-0.0170	0.0098	10	10	2.29	-	[42]
298.15	-0.0407	-0.0293	0.0283	8	8	4.73	-	[44]
298.15	-0.0345	-0.0226	0.0395	18	18	3.43	-	[42+44]
303.15	-0.0367	-0.0311	0.0620	18	18	3.60	-	[42]
313.15	-0.0706	-0.0674	0.1052	18	18	5.43	-	[42]
323.15	-0.2565	-0.0862	0.0031	8	8	1.65	0.16	This work
333.15	-0.2144	-0.0561	0.0070	9	9	2.58	0.27	This work
343.15	-0.2031	-0.0341	0.0176	11	11	3.36	0.30	This work
343.20	-0.0705	-0.0553	0.0083	9	9	2.57	-	[45]
353.15	-0.2198	-0.0370	0.0097	11	11	2.64	0.23	This work
353.20	-0.0639	-0.0352	0.0062	7	7	2.33	-	[45]

4.4. PR and SRK semi-prediction results

Finally, we calculated the critical curves and isotherms for the carbon dioxide + 1,4-dioxane system using the average values of optimal BIPs obtained using the critical parameters and acentric factors from DIPPR [68] for each EoS, but excluding the two sets reported in Ref. [45]. These parameters are k_{12} = -0.1479 and l_{12} = -0.0478 for the SRK EoS

and k_{12} = -0.1362 and l_{12} = -0.0475 for the PR EoS, respectively. The predicted critical curves with these sets of parameters are shown in **Fig. 9 (a)** and detailed in **Fig. 9 (b)**. The calculations by PR with k_{12} = -0.05 and l_{12} = -0.05 and pure components parameters from the same source [68] as for the other two models are also included in the same figures (**Fig. 9 (a), (b)**). The critical pressures are overlaping for both SRK and PR with averaged values of BIPs for pressures smaller than the CPM, which is better predicted by PR in comparison with our data, but still overestimating the experimental data, and the differences become noticeable towards the critical point of 1,4-dioxane. When comparing with the results by PR with k_{12} = -0.05 and l_{12} = -0.05, besides the different type of phase behavior, the CPM is shifted to the right and reproduces better the experimental data reported by [43]. In **Fig. 10**, the pressure-composition projection of the global phase diagram calculated using the same models are shown. The prediction results are very good for both SRK and PR with averaged binary interaction parameters, while for PR with k_{12} = -0.05 and l_{12} = -0.05, the critical compositions are underestimated. Further, the new critical experimental data are compared with the model calculations in **Fig. 11** and detailed in **Fig. 12,** which plots the critical temperatures against critical compositions. SRK EoS performs slightly better than PR EoS, with average values of the optimal BIPs. The new data and all literature isothermal data are compared with predictions by SRK (with k_{12} = -0.1362 and l_{12} = -0.0475) and PR (with k_{12} = -0.1479 and l_{12} = -0.0478) in **Figs. 13** and **14,** respectively. At lower temperatures, the models predict higher solubilities than the experimental ones, while at higher temperatures they underestimate the compositions.

Conclusions

New isothermal vapor–liquid equilibrium and critical data for the carbon dioxide + 1,4-dioxane binary system were measured using a visual high-pressure static-analytic setup. The measurements were performed at 323.15 K, 333.15 K, 343.15 K, and 323.15 K and pressures up to 122.7 bar. The critical curve (pressure – temperature – composition) was also determined at pressures up to 158.8 bar and temperatures up to 420.15 K.

The Soave–Redlich–Kwong and Peng–Robinson equations of state coupled with classical van der Waals mixing rules were used to model the phase behavior of this system. The influence of critical parameters and acentric factors of pure components from several database/sources was studied. As the differences among the critical parameters and acentric factors considered for both carbon dioxide and 1.4-dioxane are small, no significant influence

was observed. The calculation results by the two models were compared with the new experimental and previous literature data for carbon dioxide + 1,4-dioxane system. Both models predicted reasonably well the phase behavior of the carbon dioxide + 1,4-dioxane system.

Acknowledgement

„This work was supported by a grant of Ministry of Research and Innovation, CNCS - UEFISCDI, project number PN-III-P4-ID-PCE-2016-0629, within PNCDI III".

References

[1] http://altgreensolv.chfiz.pub.ro/PN-III-P4-ID-PCE-2016-0629_EN.html, accessed March 2021.

[2] J. G. Anderson, C. E. Clapp, Phys. Chem. Chem. Phys. 20 (2018) 10569.

[3] S. D. Kenarsari, D. Yang, G. Jiang, S. Zhang, J. Wang, A. G. Russell, Q. Wei, M. Fan, RSC Adv. 3 (2013) 22739.

[4] C. Secuianu, V. Feroiu, D. Geană, J. Chem. Eng. Data 48 (2003) 1384.

[5] C. Secuianu, V. Feroiu, D. Geană, Rev. Chim. (Bucharest) 54 (2003) 874.

[6] C. Secuianu, V. Feroiu, D. Geană, J. Chem. Eng. Data 49 (2004) 1635.

[7] C. Secuianu, V. Feroiu, D. Geană, Rev. Chim. (Bucharest) 58 (2007) 1176.

[8] C. Secuianu, V. Feroiu, D. Geană, Fluid Phase Equilib. 270 (2008) 109.

[9] C. Secuianu, V. Feroiu, D. Geană, J. Chem. Eng. Data 53 (2008) 2444.

[10] C. Secuianu, V. Feroiu, D. Geană, J. Supercritical Fluids 47 (2008) 109.

[11] C. Secuianu, V. Feroiu, D. Geană, Rev. Chim. (Bucharest) 60 (2009) 472.

[12] C. Secuianu, V. Feroiu, D. Geană, Cent. Eur. J. Chem. 7 (2009) 1.

[13] C. Secuianu, V. Feroiu, D. Geană, J. Chem. Eng. Data 54 (2009) 1493.

[14] C. Secuianu, V. Feroiu, D. Geană, J. Supercrit. Fluid 55 (2010) 653.

[15] C. Secuianu, V. Feroiu, D. Geană, J. Chem. Thermodyn. 42 (2010) 1286.

[16] C. Secuianu, V. Feroiu, D. Geană, J. Chem. Eng. Data 56 (2011) 5000.

[17] S. Secuianu, J. Qian, R. Privat, J.-N Jaubert, Ind. Eng. Chem. Res. 51 (2012) 11284.

[18] S. Sima, S. Ioniță, C. Secuianu, V. Feroiu, D. Geană, Rev. Chim. (Bucharest) 65 (2014) 272.

[19] S. Sima, C. Secuianu, V. Feroiu, D. Geană, Cent. Eur. J. Chem. 12 (2014) 893.

[20] S. Sima, C. Secuianu, V. Feroiu, D. Geană, Cent. Eur. J. Chem. 12 (2014) 953.

[21] S. Ioniţă, C. Secuianu, V. Feroiu, D. Geană, U.P.B. Sci. Bull. Series B 77 (2015) 31.

[22] C. Secuianu, S. Ioniţă, V. Feroiu, D. Geană, J. Chem. Thermodyn. 93 (2016) 360.

[23] C. Secuianu, V. Feroiu, D. Geană, Fluid Phase Equilib. 428 (2016) 62.

[24] S. Sima, R.C. Racoviţă, C. Dincă, V. Feroiu, C. Secuianu, U.P.B. Sci. Bull. Series B 79 (2017) 11.

[25] S. Sima, S. Ioniţă, C. Secuianu, V. Feroiu, D. Geană, J. Chem. Eng. Data 63 (2018) 1109.

[26] S. Sima, C. Secuianu, V. Feroiu, S. Ioniţă, D. Geană, Fluid Phase Equilib. 510 (2020) 112487.

[27] C. Secuianu, V. Feroiu, D. Geană, Fluid Phase Equilib. 261 (2007) 337.

[28] C. Secuianu, V. Feroiu, D. Geană, J. Chem. Eng. Data 55 (2010) 4255.

[29] S. Sima, J. Cruz-Doblas, M. Cismondi, C. Secuianu. Cent. Eur. J. Chem. 12 (2014) 918.

[30] A. Crişciu, S. Sima, A. S. Deaconu, A. Chirilă, D. Deaconu, C. Secuianu, V. Feroiu, Rev. Chim. (Bucharest) 67 (2016) 1984.

[31] S. Sima, J. M. Milanesio, J. I. Ramello, M. Cismondi, C. Secuianu, V. Feroiu, D. Geană, J. Chem. Thermodyn. 93 (2016) 374.

[32] S. Sima, C. Secuianu, V. Feroiu, Fluid Phase Equilib. 458 (2018) 47.

[33] S. Sima, R. C. Racoviţă, A. Chirilă, D. Deaconu, V. Feroiu, C. Secuianu, Stud. Univ. Babes-Bolyai Chem. 64 (2019) 129.

[34] S. Sima, A. C. Vărzaru, R. C. Racoviţă, V. Feroiu, C. Secuianu, Phase equilibria in systems of CO_2 and esters, 21st Romanian Int. Conf. Chem. Chem. Eng. – RICCCE 21, Mamaia-Constanţa, Romania, 4-7 September 2019.

[35] G. M. Kontogeorgis**,** R. Dohrn, I. G. Economou, J.-C. de Hemptinne, A. ten Kate, S. Kuitunen, M. Mooijer, L. Fele Žilnik, V. Vesovic, Ind. Eng. Chem. Res. 60 (2021) 4987.

[37] R. Dohrn, G. Brunner, Fluid Phase Equilib. 106 (1995) 213.

[38] M. Christov, R. Dohrn, Fluid Phase Equilib. 202 (2002) 153.

[39] R. Dohrn, S. Peper, J. M. S. Fonseca, Fluid Phase Equilib. 288 (2010) 1.

[40] J. M. S. Fonseca, R. Dohrn, S. Peper, Fluid Phase Equilib. 300 (2011) 1.

[41] S. Peper, J.M.S. Fonseca, R. Dohrn, Fluid Phase Equilib. 484 (2019) 126.

[42] A. Kordikowski, A. P. Schenk, R. M. van Nielen, C. J. Peters, Fluid Phase Equilib. 8 (1995) 205.

[43] T. L. Chester, B. S. Haynes, J. Supercrit. Fluids 11 (1997) 15.

[44] M. B. Miller, D.-L. Chen, D. R. Luebke, J. K. Johnson, R. M. Enick, J. Chem. Eng. Data 56 (2011) 1565.

[45] A. H. Tiwikrama, Afrianto, H.-Y. Chiu, D.-Y. Peng, H.-m. Lin, M.-J. Lee, J. Chem. Thermodynamics 136 (2019) 141.

[46] https://www.epa.gov/sites/production/files/2014-03/documents/ffrro_factsheet_contaminant_14-dioxane_january2014_final.pdf, accessed March 2021.

[47] M. Zhang, M.-L. Ge, Y.-H. Jiao, Z. Mua, R. Huang, Z.-Z. He, J. Chem. Thermodynamics 129 (2019) 92.

[48] A. S. Reis Machado, R. M. A. Sardinha, E. G. de Azevedo, M. N. da Ponte, J. Supercrit. Fluid. 7 (1994) 87.

[49] M. J. Lazzaroni, D. Bush, R. Jones, J. P. Hallett, C. L. Liotta, C. A. Eckert, Fluid Phase Equilib. 224 (2004) 143.

[50] Y. Li, Y. Mou, Y. Zhu, J. Liu, Jing Liu, H. Zhao, J. Chem. Thermodyn. 149 (2020) 106170.

[51] H. Pahlavanzadeh, A. Kamran-Pirzaman, Amir H. Mohammadi, Fluid Phase Equilib. 320 (2012) 32.

[52] T. Maekawa, Fluid Phase Equilib. 384 (2014) 95.

[53] D. M. Kassim, H. A. Zainei, S. A. Al-Asaf, E. K. Talib, Fluid Phase Equilib. 41 (1988) 287.

[54] S. Peper, R. Dohrn, J. Supercrit. Fluid, 66 (2012) 2.

[55] G. Soave, Chem. Eng. Sci. 27 (1972) 1197.

[56] D. Y. Peng, D. B. Robinson, Ind. Eng. Chem. Fundam. 15 (1976) 59.

[57] P. H. van Konynenburg, R. L. Scott, Trans. R. Soc. London, Ser. A 298 (1980) 495.

[58] R. Privat, J. N. Jaubert, Chem. Eng. Res. Des. 91 (2013) 1807.

[59] S. Sima, V. Feroiu, D. Geană, J. Chem. Eng. Data 56 (2011) 5052.

[60] P. Guilbot, A. Valtz, H. Legendre, D. Richon, Analusis 28 (2000) 426.

[61] E.-J. Choi, S.-D. Yeo, J. Chem. Eng. Data 43 (1998) 714.

[62] A. Pina-Martinez, R. Privat, J.-N. Jaubert, D.-Y. Peng, Fluid Phase Equilib. 485 (2019) 264.

[63] DETHERM Database (DECHEMA Chemistry Data Series, Frankfurt, Germany, 1991–2014).

[64] R. C. Reid, J. M. Prausnitz, B. E. Poling, The Properties of Gases and Liquids, 4th Ed., McGraw-Hill, New York, 1987.

[65] B. E. Poling, J. M. Prausnitz, J. P. O'Connell, The Properties of Gases and Liquids, 5th Ed., McGraw-Hill Education, New York, 2001.

[66] https://www.nist.gov/srd/refprop

[67] C.L. Yaws, Chemical Properties Handbook, McGraw-Hill, New York, 1999.

[68] Evaluated Standard Thermophysical Property Values, DIPPR Project 801 full version, Brigham Young University, Provo Utah, 2005.

[69] J.-N. Jaubert, Y. Le Guennec, A. Pina-Martinez, N. Ramirez-Velez, S. Lasala, B. Schmid, I. K. Nikolaidis, I. G. Economou, R. Privat, Ind. Eng. Chem. Res. 59 (2020) 14981.

[70] D. Geană, L. Rus, Phase equilibria database and calculation program for pure components systems and mixtures, in Proc. Romanian Int. Conf. Chem. Chem. Eng. (RICCCE XIV), Bucharest, Romania, 2, 170–178, 2005.

[71] http://gpec.phasety.com, accessed 2016.

[72] R. A. Heidemann, A. M. Khalil, AIChE J. 26 (1980) 769.

[73] R. Stockfleth, R. Dohrn, Fluid Phase Equilib. 145 (1998) 43.

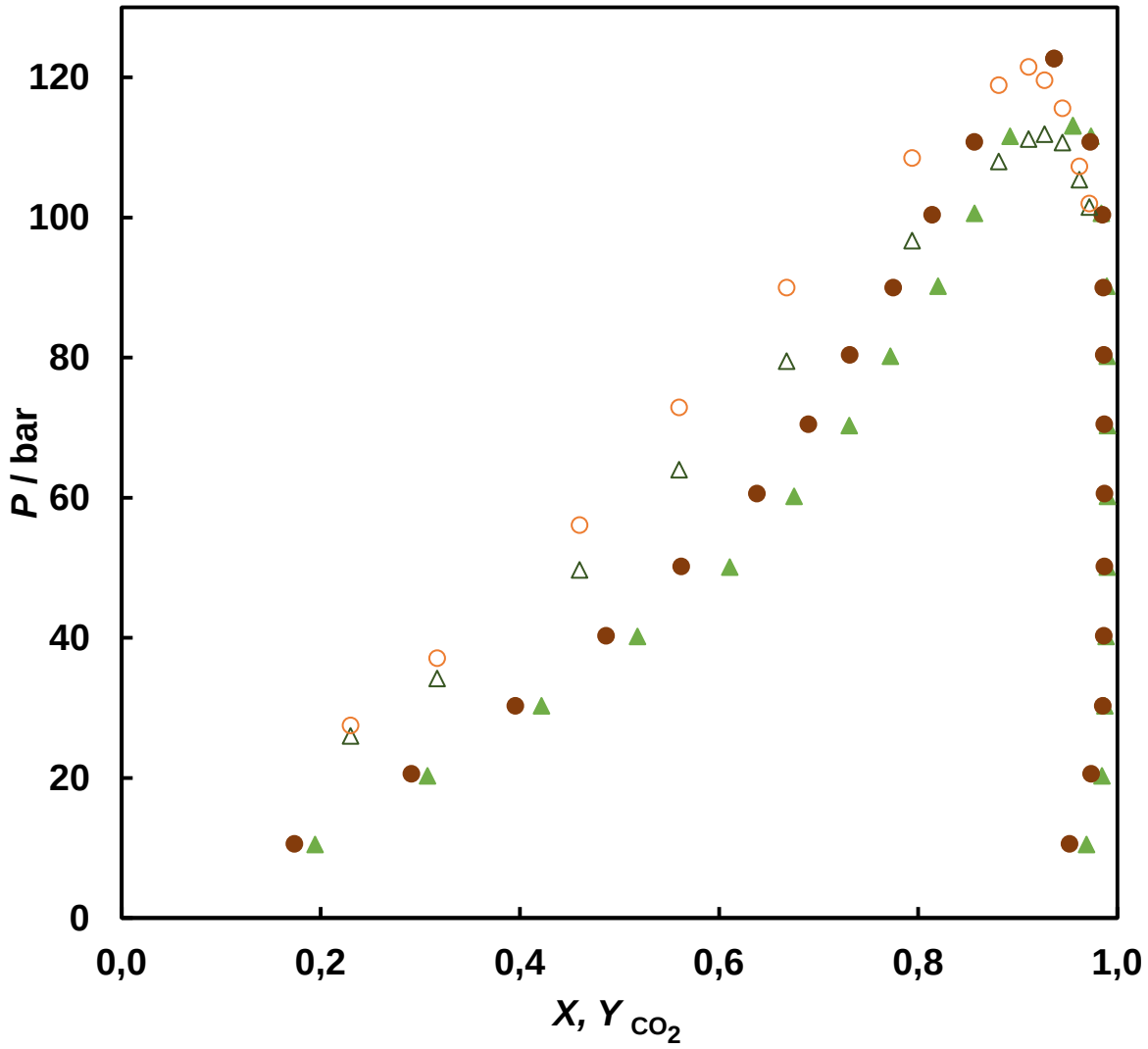

Fig. 2. Comparison of measured and literature data for carbon dioxide (1) + 1,4-dioxane (2) system: ▲, 343.15 K, this work; Δ, 343.20 K, [45]; ●, 353.15 K, this work; ○, 353.20 K, [45].

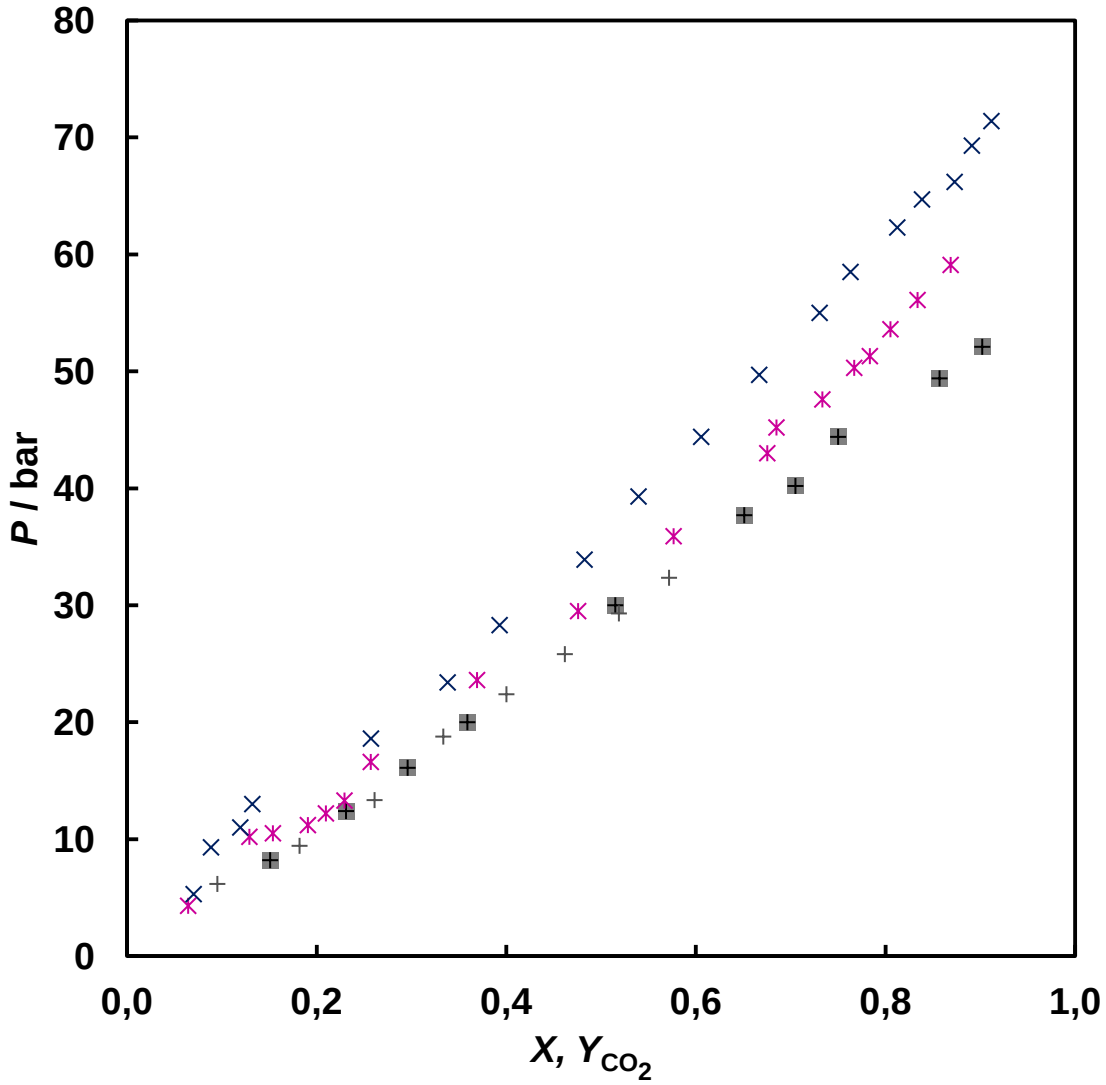

Fig. 3. Comparison of literature data for carbon dioxide (1) + 1,4-dioxane (2) system: +, 298.15 K, [44]; ■, 298.15 K, [42]; *, 303.15 K, [42]; ×, 313.15 K, [42].

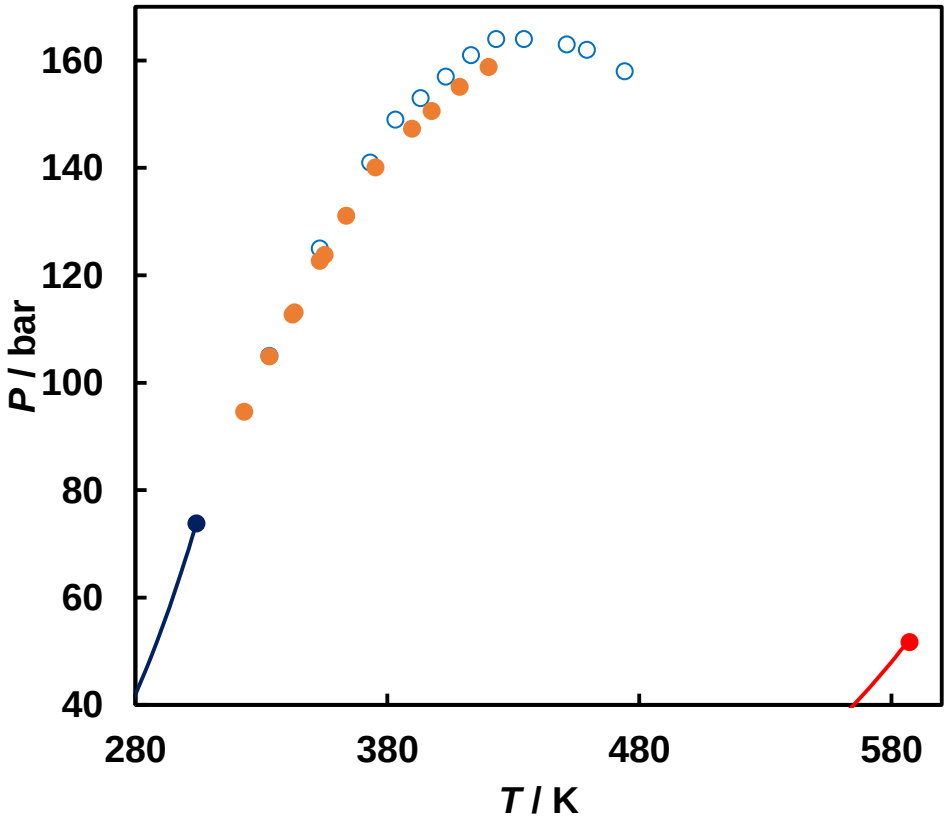

Fig. 4. *P–T* fluid phase diagram of the carbon dioxide (1) + 1,4-dioxane system: ●, critical point of CO*2*; ●, critical point of 1,4-dioxane; −, vapor pressure of CO_2; −, vapor pressure of 1,4-dioxane; ●, this work; ○, Chester and Haynes [43].

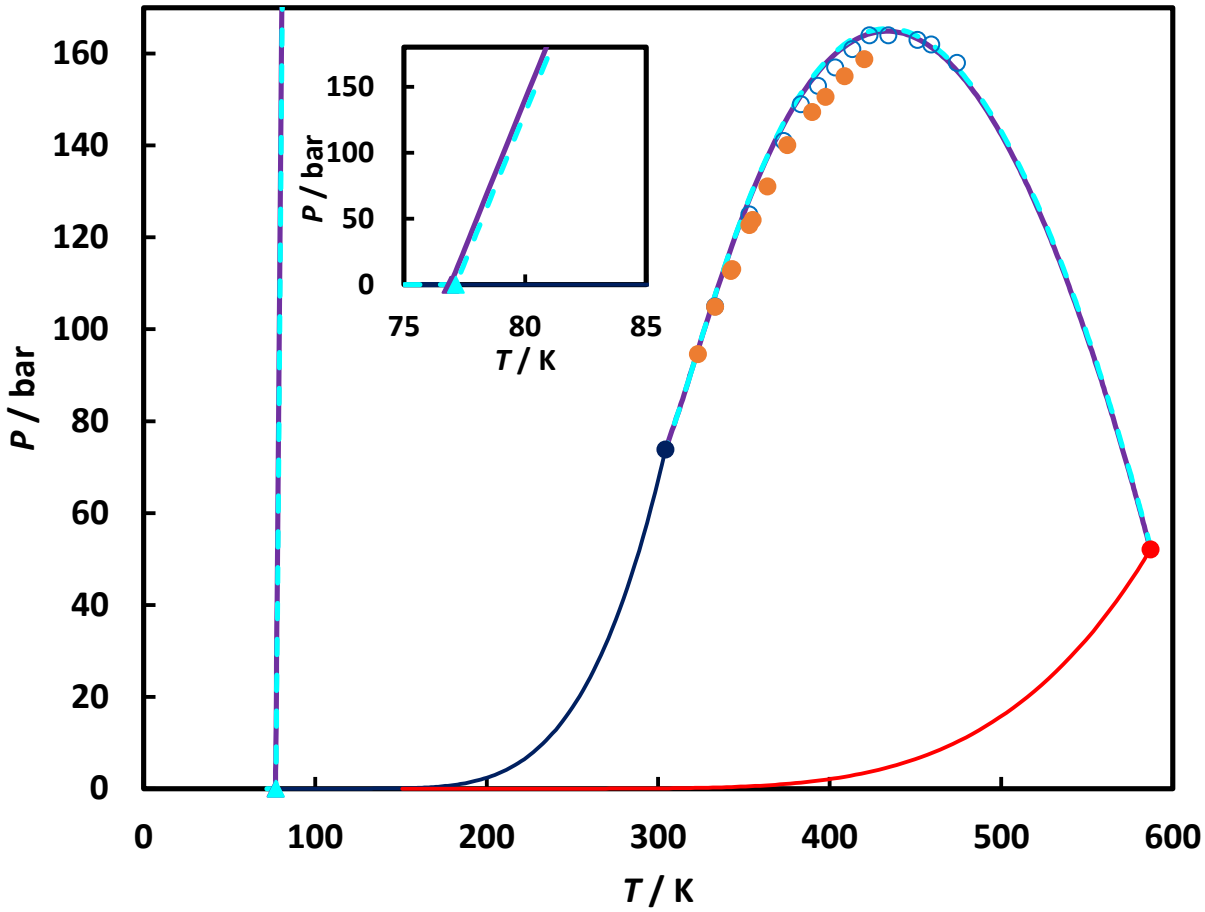

Fig. 5. *P–T* fluid phase diagram of the carbon dioxide (1) + 1,4-dioxane system: ●, critical point of CO_2; ●, critical point of 1,4-dioxane; –, vapor pressure of CO_2; –, vapor pressure of 1,4-dioxane; ●, this work; ○, Chester and Haynes [43]; ▬, critical lines, and ▲, UCEP, PR (-0.05; -0.05) and pure components critical parameters and acentric factors from [68]; - - - , critical lines and ▲, UCEP, PR (-0.05; -0.05) and pure components critical parameters and acentric factors from [42]. Detail of the L-L critical curves and UCEPs.

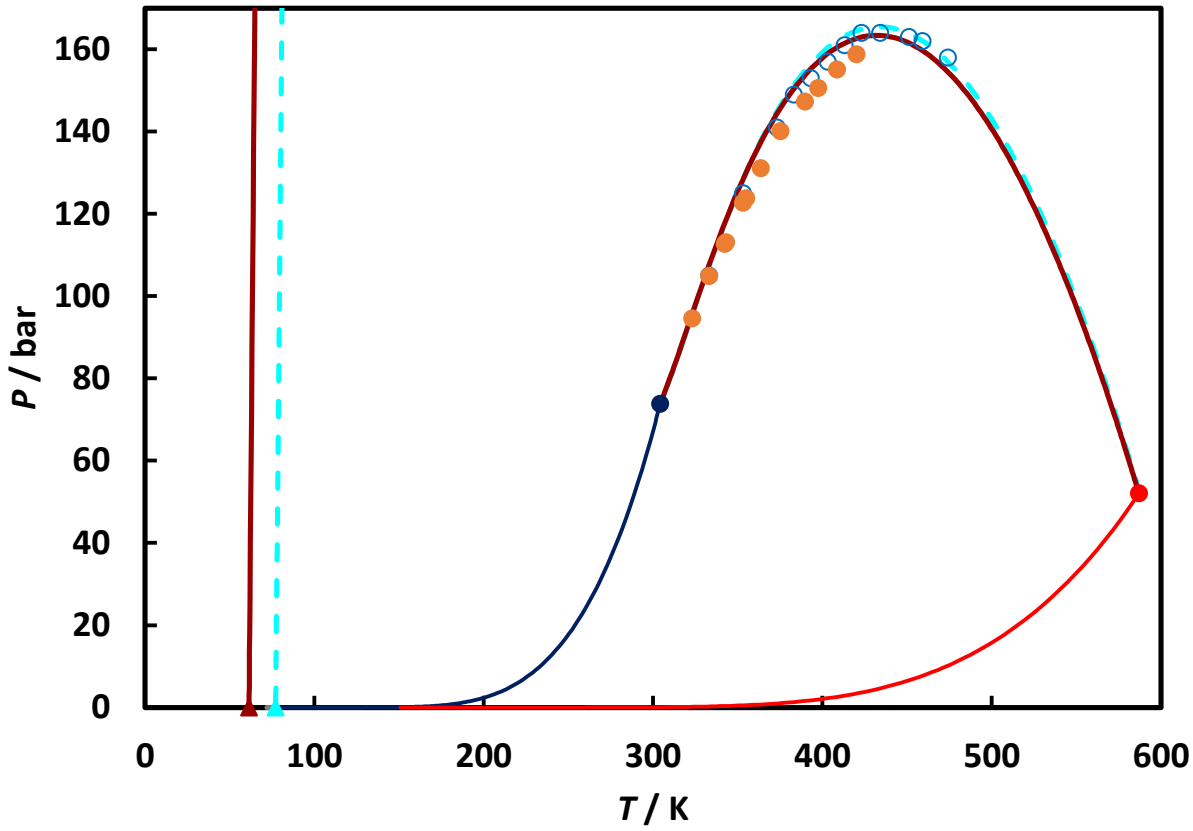

Fig. 6. *P*–*T* fluid phase diagram of the carbon dioxide (1) + 1,4-dioxane system: ●, critical point of CO_2; ●, critical point of 1,4-dioxane; −, vapor pressure of CO_2; −, vapor pressure of 1,4-dioxane; ●, this work; ○, Chester and Haynes [43]; ▬, critical lines, and ▲, UCEP, PR (-0.0606; -0.0475) and pure components critical parameters and acentric factors from [45]; - - - , critical lines and ▲, UCEP, PR (-0.05; -0.05) and pure components critical parameters and acentric factors from [42].

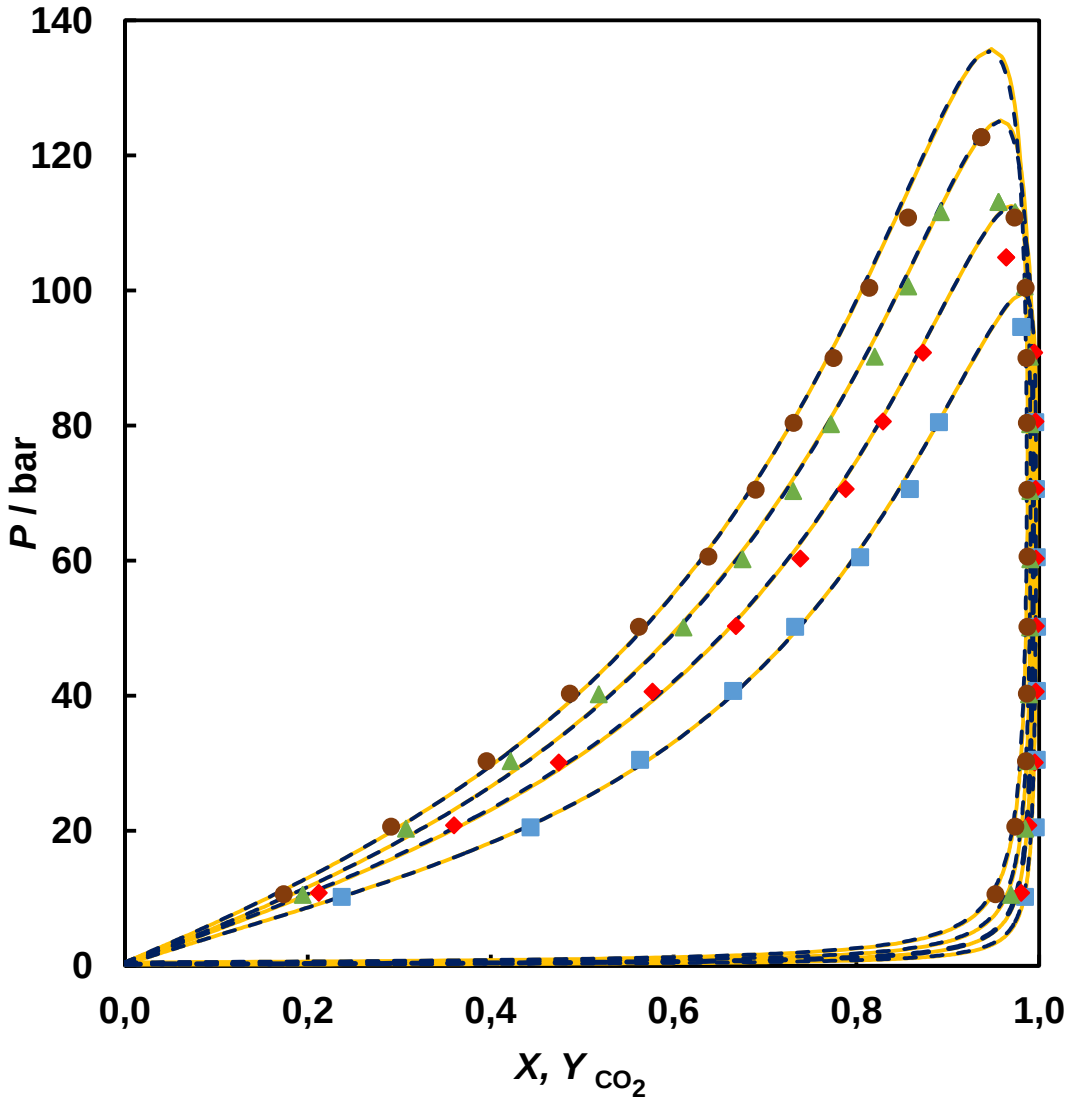

Fig. 7. Comparison of new data and calculations SRK, and PR EoSs for carbon dioxide (1) + 1,4-dioxane (2) binary system with pure components parameters from DIPPR [68]: ■, 323.15 K; ♦, 333.15 K; ▲, 343.15 K; ●, 353.15 K; ---, PR/2PCMR; ─, SRK/2PCMR.

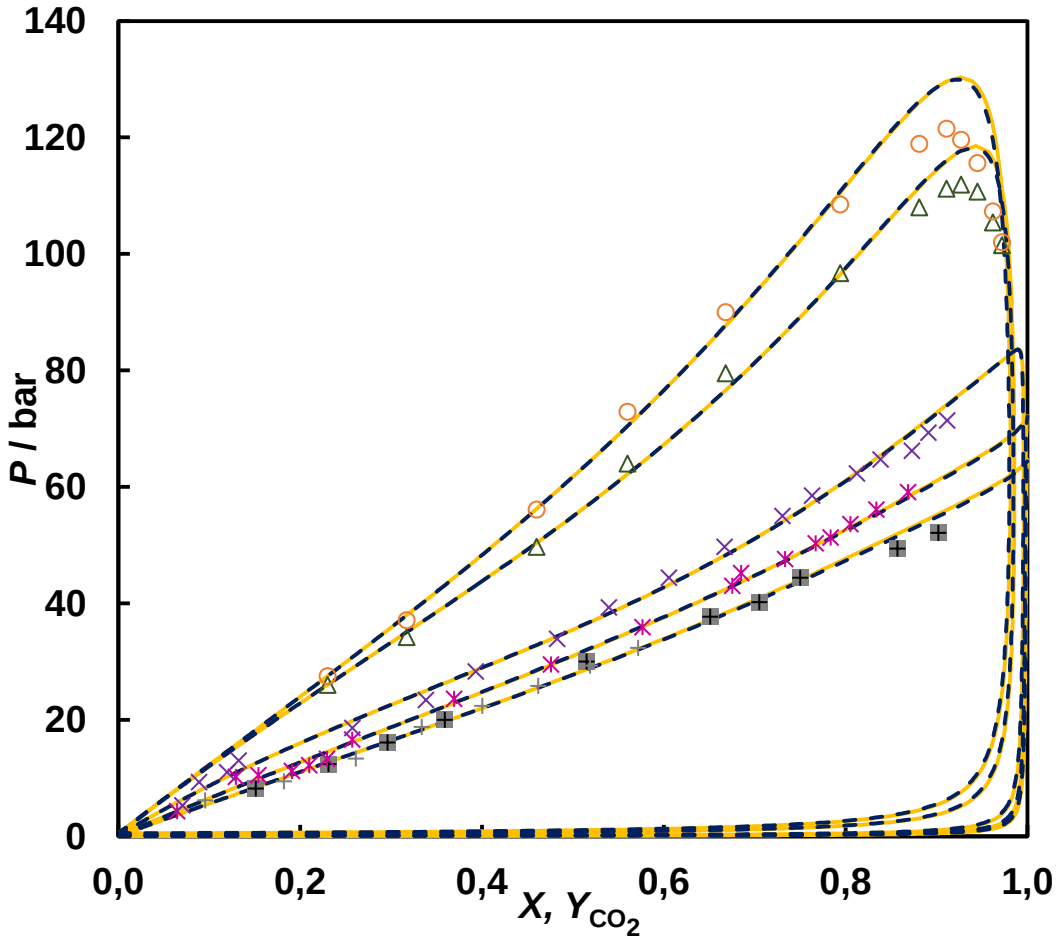

Fig. 8. Comparison of literature data and calculations by SRK, and PR EoSs for carbon dioxide (1) + 1,4-dioxane (2) system with pure components parameters from DIPPR [68]: +, 298.15 K, [44]; ■, 298.15 K, [42]; *, 303.15 K, [42]; ×, 313.15 K, [42]; Δ, 343.20 K, [45]; ○, 353.20 K, [45]; ---, PR/2PCMR; –, SRK/2PCMR.

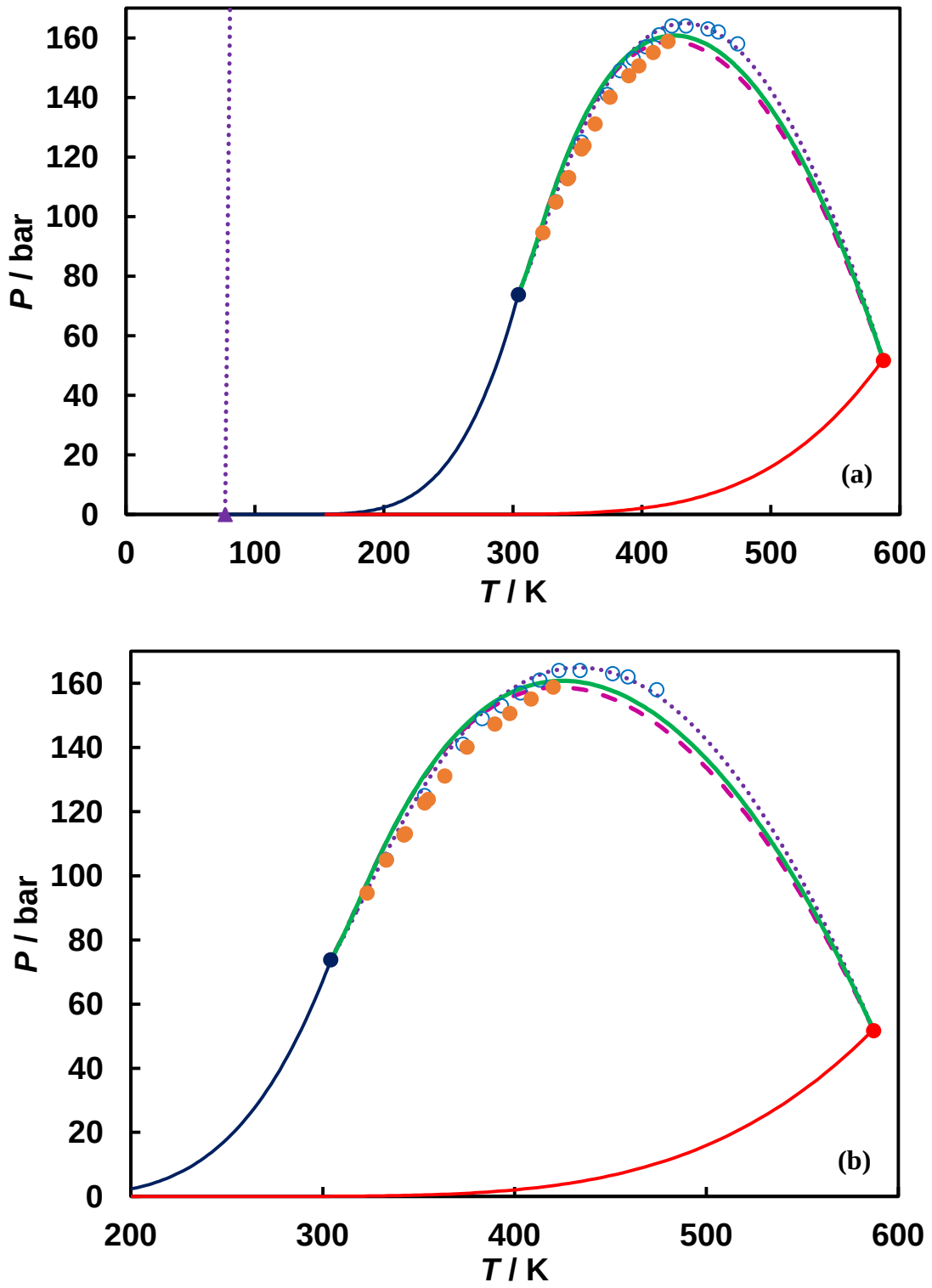

Fig. 9. *P–T* fluid phase diagram of the carbon dioxide (1) + 1,4-dioxane system. (**a**) ●, critical point of CO_2; ●, critical point of 1,4-dioxane; –, vapor pressure of CO_2; –, vapor pressure of 1,4-dioxane; ●, this work; ○, Chester and Haynes [44]; ····, critical lines, and ▲, UCEP, PR (-0.05; -0.05); - - -, PR (-0.1362; -0.0475); ▬, SRK (-0.1479; -0.0478). (**b**). Enhancement of the L-V critical curve.

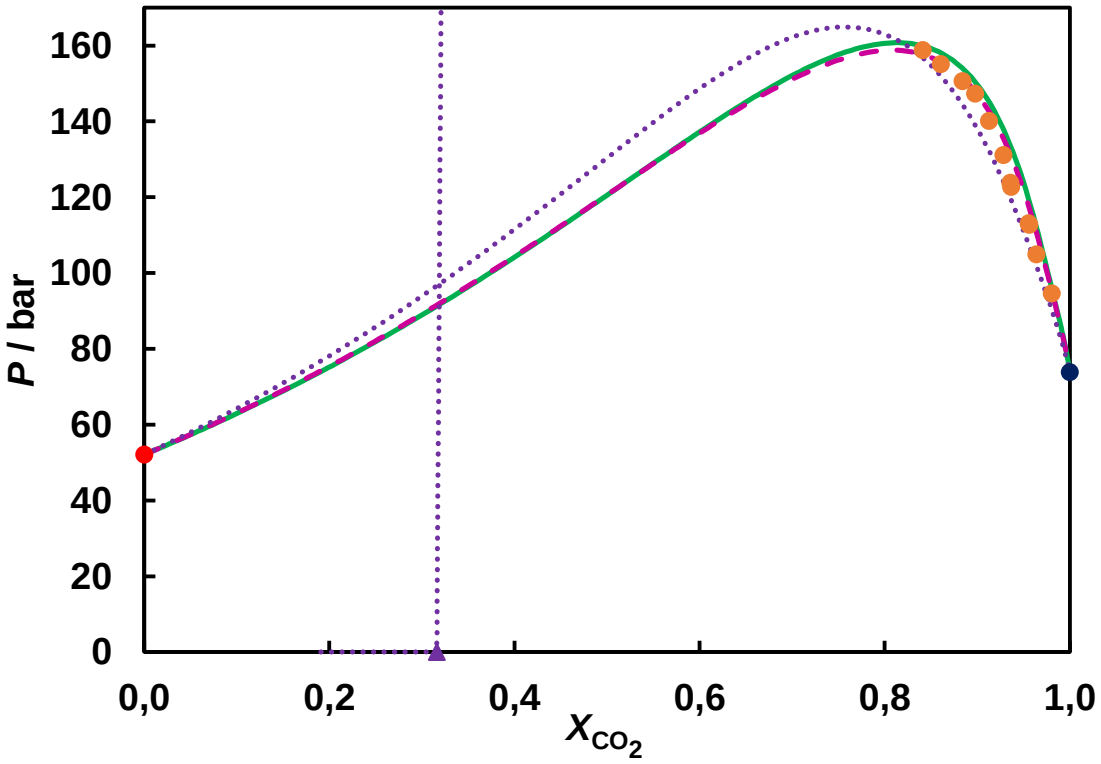

Fig. 10. *P–X* fluid phase diagram of the carbon dioxide (1) + 1,4-dioxane system: ●, critical point of CO_2; ●, critical point of 1,4-dioxane; –, vapor pressure of CO_2; –, vapor pressure of 1,4-dioxane; ●, this work; ····, critical lines, and ▲, UCEP, PR (-0.05; -0.05); - - -, PR (-0.1362; -0.0475); ▬, SRK (-0.1479; -0.0478).

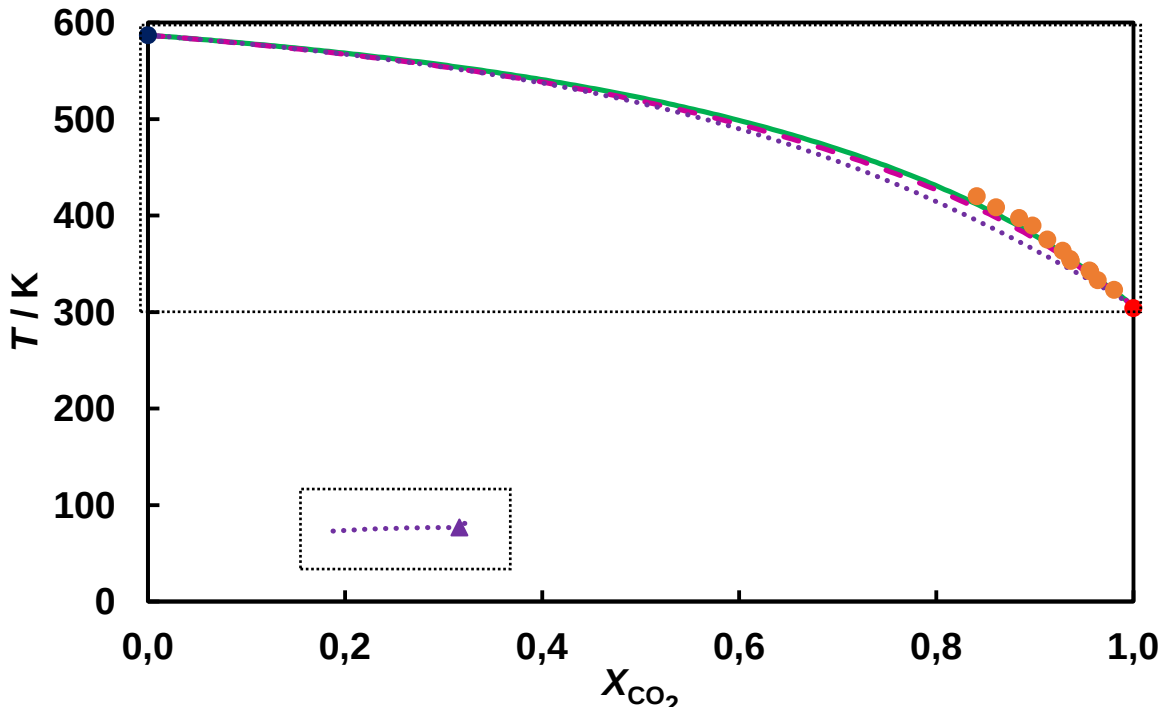

Fig. 11. *T*–*X* fluid phase diagram of the carbon dioxide (1) + 1,4-dioxane system: ●, critical point of CO_2; ●, critical point of 1,4-dioxane; –, vapor pressure of CO_2; –, vapor pressure of 1,4-dioxane; ●, this work; ····, critical lines, and ▲, UCEP, PR (-0.05; -0.05); - - -, PR (-0.1362; -0.0475); ▬, SRK (-0.1479; -0.0478).

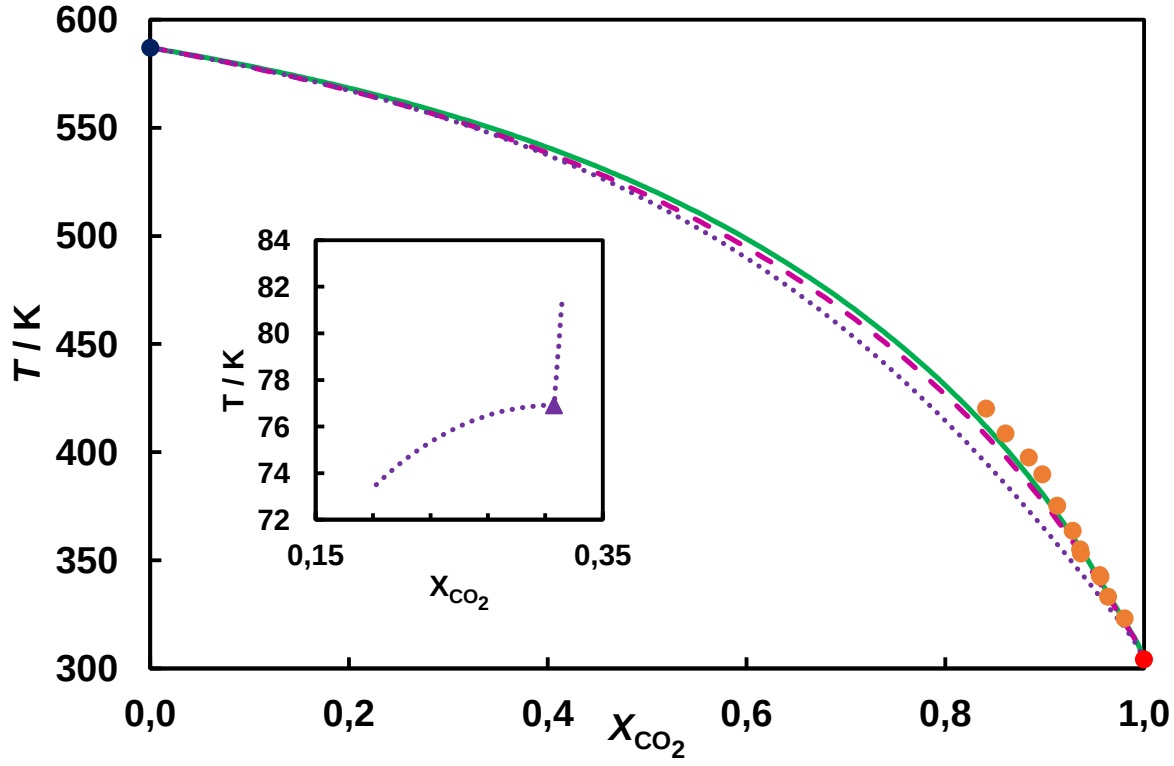

Fig. 12. Enhancements of the two selected areas of the *T*–*X* fluid phase diagram of the carbon dioxide (1) + 1,4-dioxane system from **Fig. 11**.

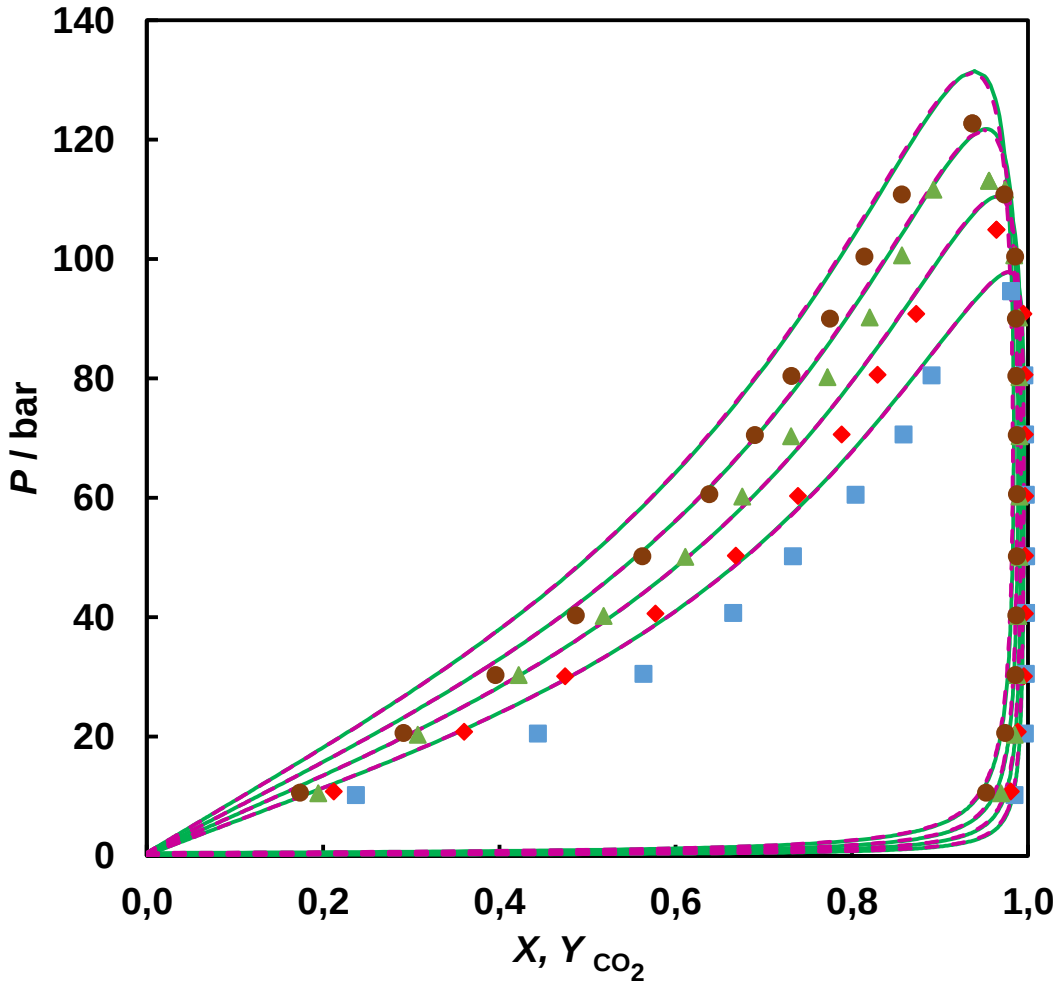

Fig. 13. Comparison of new data and predictions by PR and SRK EoSs for carbon dioxide (1) + 1,4-dioxane (2) binary system: ■, 323.15 K; ♦, 333.15 K; ▲, 343.15 K; ●, 353.15 K; - - -, PR (-0.1362; -0.0475); —, SRK (-0.1479; -0.0478).

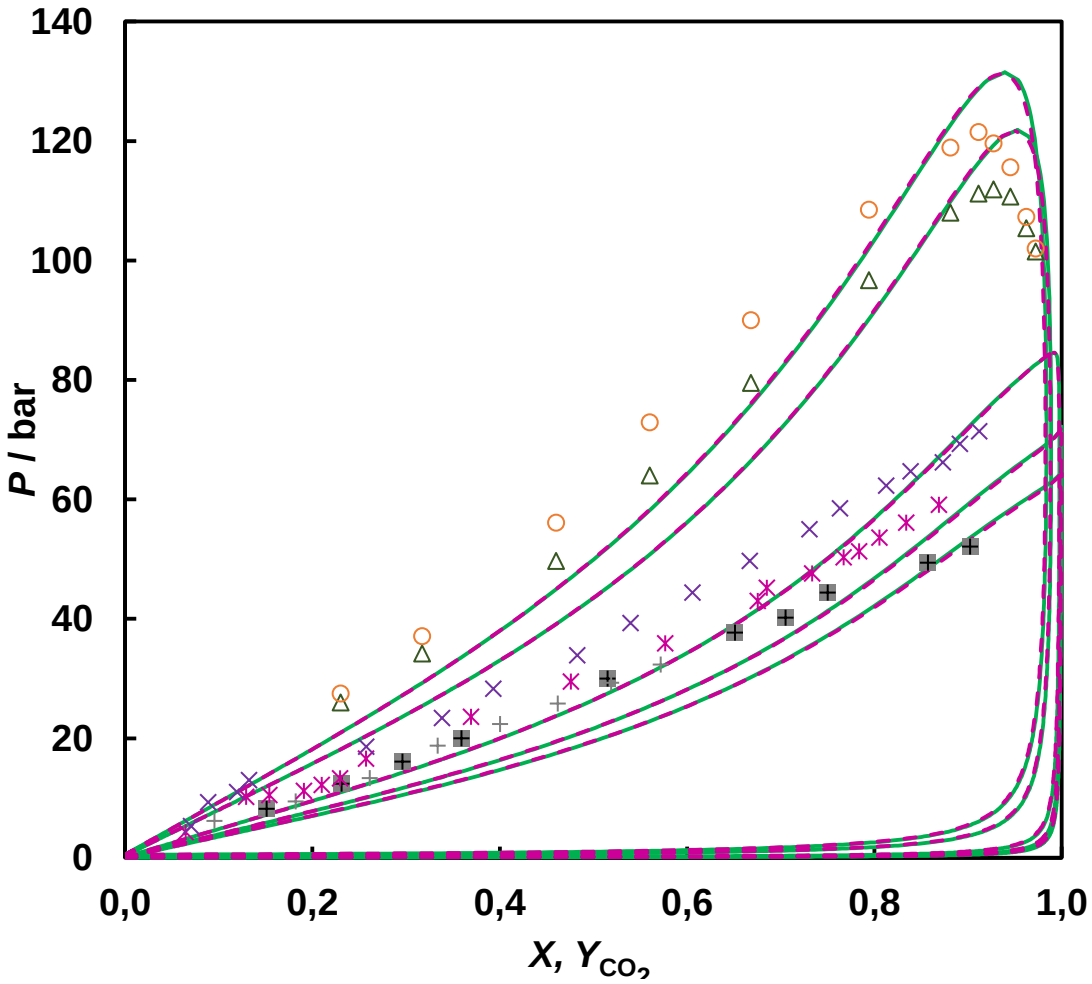

Fig. 14. Comparison of literature data and predictions by PR and SRK EoSs for carbon dioxide (1) + 1,4-dioxane (2) system: +, 298.15 K, [44]; ▪, 298.15 K, [42]; *, 303.15 K, [42]; ×, 313.15 K, [42]; Δ, 343.20 K, [45]; ○, 353.20 K, [45]; - - -, PR (-0.1362; -0.0475); ▬, SRK (-0.1479; -0.0478).